Hindawi
Geofluids
Volume 2021, Article ID 6617211, 10 pages
https://doi.org/10.1155/2021/6617211

Research Article

Comprehensive Evaluation of Waterflooding Performance with Induced Fractures in Tight Reservoir: A Field Case

Naichao Feng,[1] Yuwen Chang,[1] Zuoqian Wang,[1] Tao Liang,[1] Xiaofei Guo,[1] Yimeng Zhu,[1] Limin Hu,[2] and Yang Wang[2]

[1]*Research Institute of Petroleum Exploration & Development, PetroChina, 100083 Beijing, China*
[2]*China University of Petroleum, Beijing and State Key Laboratory of Petroleum Resources and Prospecting, Beijing, China*

Correspondence should be addressed to Yang Wang; petroyang@163.com

Received 21 December 2020; Revised 18 January 2021; Accepted 12 February 2021; Published 24 February 2021

Academic Editor: Qingquan Liu

Whether intentionally or unintentionally, waterflooding always takes place under fracturing condition in tight reservoir because of the extremely limited water absorption ability of the formation. Recently, we proposed a novel workflow, including real-time monitoring, formation testing analysis, and dynamic production analysis, to timely and effectively identify the initiation of waterflood-induced fractures (WIFs) and characterize the waterflooding behaviors for a well group. In this paper, we further provide a supplementary study to evaluate the waterflooding performance from the well group to the field basis. The utilization factor (UF) is first estimated on the basis of injection/production data by material balance theory, which provides an overall picture of water injection efficiency every year. Then, the areal (straightforwardly showed by water cut and formation pressure distributions) and vertical sweep (includes the water absorption in injectors and water breakthrough in producers) behaviors are studied to investigate the waterflooding characteristics and residual oil distributions. Lastly, three key influence factors are detailedly discussed: sand body connectivity, WIFs, and injection and production correspondence. Combining the previous work for the single well group, and the study in this paper to field basis, one can have a better and much more comprehensive understanding of the waterflooding performance and then thus take the corresponding adjustment measurements to improve waterflooding effectiveness.

1. State of Problem

Block D is a typical tight oil reservoir in Changqing Oil field, China. It was put into production in 1995, and the advanced water injection was applied in 2002 to maintain the reservoir pressure because of the low pressure coefficient. The main oil-bearing layer of this block is C61, with the average effective thickness of 15.1 m, porosity of 12.5%, and permeability of 0.54 mD. 107 infill wells were drilled in 2014, and lots of producers were converted into injectors because of the high water cut. Up to now, there are 230 producers and 63 injectors in the block. With the water cut of 48%, the oil recovery is only 10.98%, which indicates the great development potential of this field.

The waterflooding is considered to be effective in terms of reservoir pressure maintenance and oil well responses. However, lots of producers watered out very quickly and unexpectedly in the early 2014. This may be caused by WIFs, which keep closed in the original state, and then expand and extend if the reservoir pressure is larger than fracture-initiation pressure [1–4].

In order to have a better understanding of waterflooding effectiveness, a comprehensive evaluation of waterflooding performance is essential and critical. In the previous study [5–7], we proposed a novel workflow, which includes real-time monitoring, formation test, and dynamic production analysis, to characterize waterflood-induced fractures on the basis of injection/production history and formation test data for a well group.

In this paper, we extend the previous study from a well group to the field basis. We will evaluate the waterflooding performance from three aspects: UF, areal, and vertical sweep characteristics. Then, we further discuss the main factors that have a great influence on waterflooding performance.

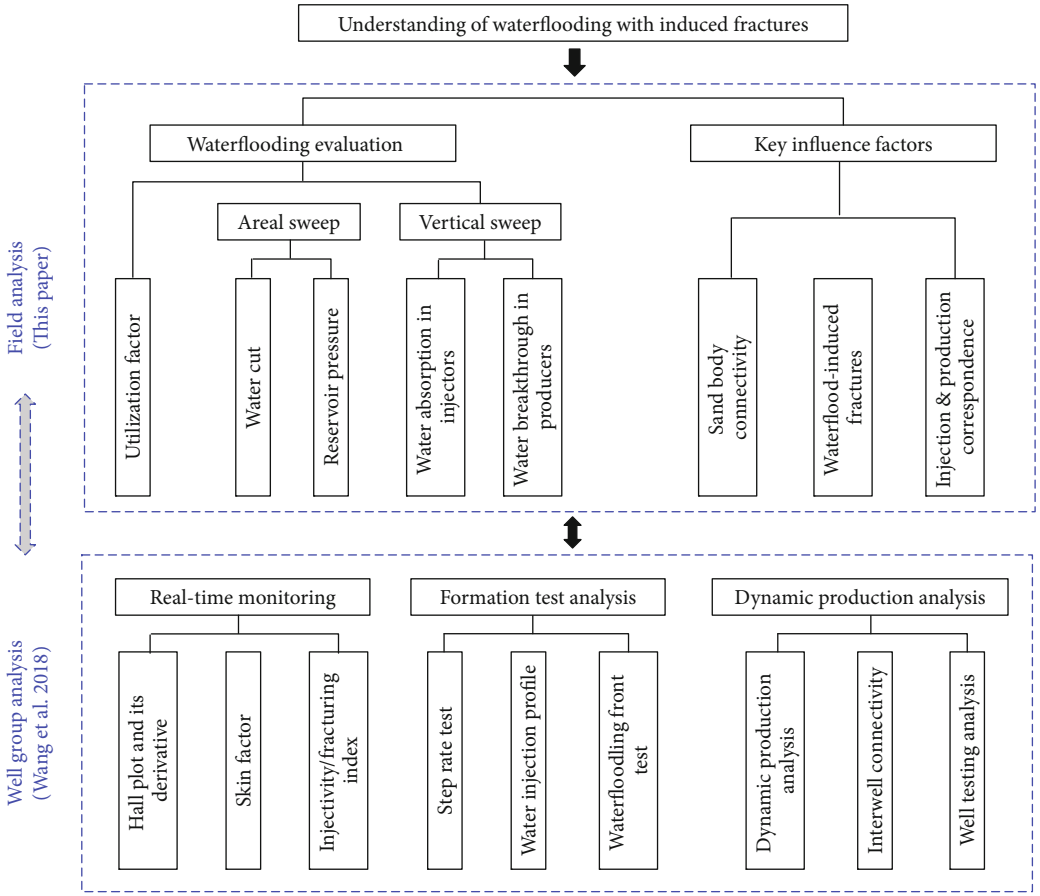

Figure 1: Integrated method for the understanding of waterflooding with the influence of induced fractures.

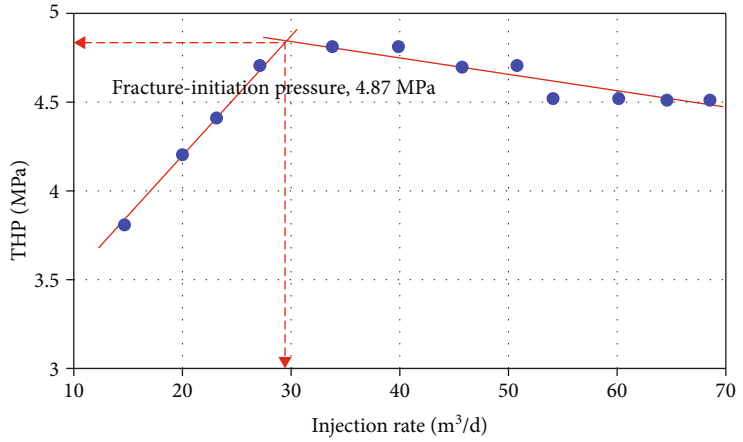

Figure 2: Step rate test of water injection well L34-30 [7].

Combining the methodology proposed in this paper and the workflow presented before [7], one can have an overall understanding of the waterflooding performance (Figure 1).

2. Raw Data Analysis

In Figure 2, we plot the tubinghead pressure (THP) vs. water injection rate for the water injection well L34-30 in this block. The THP firstly increases linearly and then slows down or even has a slightly decrease as the increase of water injection rate, which implies formation fracturing. If the inflection point THP is converted into bottom-hole pressure (BHP), the fracture-initiation pressure is obtained as about 22 MPa, which is much less than the formation breakdown pressure (30 MPa). In addition, the matching results of the shut-in pressure data for the water injection

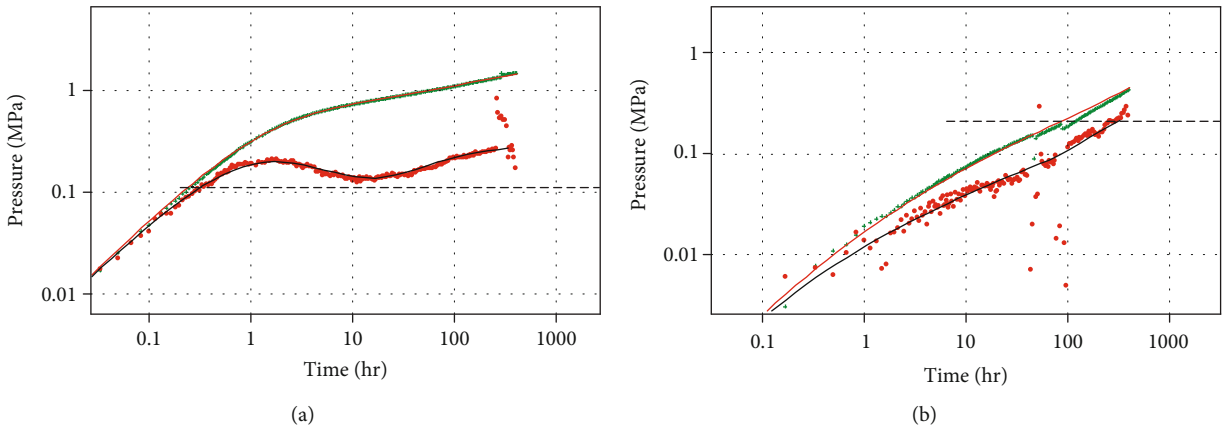

Figure 3: Matching results of BHP responses of water injection well L34-30 in (a) Mar, 2014, and (b) Jul, 2015.

Table 1: Production data of this block.

Year	Cumulative oil production (10^4m^3)	Cumulative water production (10^4m^3)	Cumulative water injection (10^4m^3)	Reservoir pressure (MPa)	Utilization factor
2009	55.06	22.99	274.52	14.07	0.315
2010	63.08	26.46	314.41	14.2	0.316
2011	70.90	30.84	345.92	13.71	0.329
2012	78.11	35.53	374.49	14.16	0.338
2013	84.77	39.75	402.00	13.25	0.348
2014	91.20	44.16	428.91	13.35	0.354
2015	97.46	48.84	456.84	12.69	0.360
2016	105.23	54.56	484.15	12.45	0.372

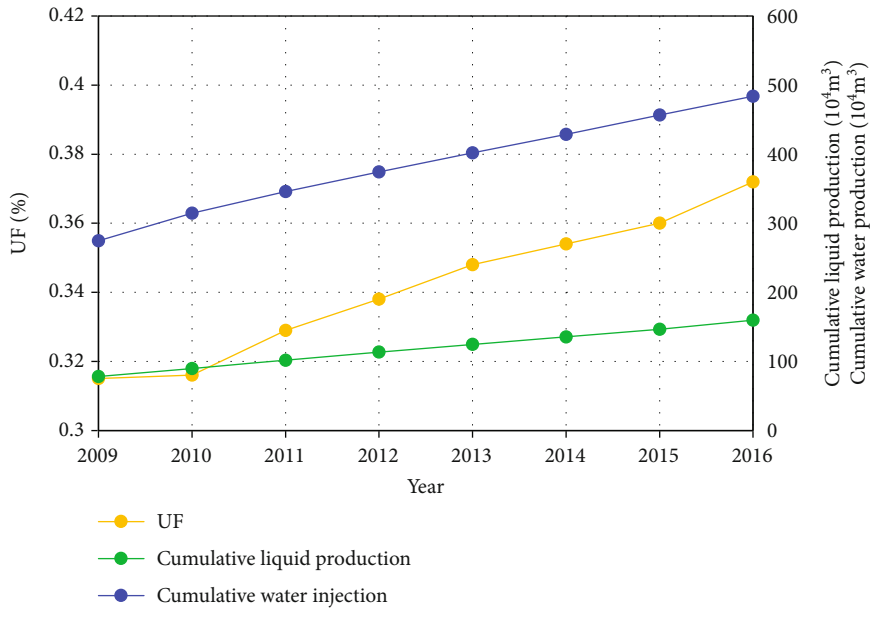

Figure 4: UF of water injection in this block from 2009 to 2016.

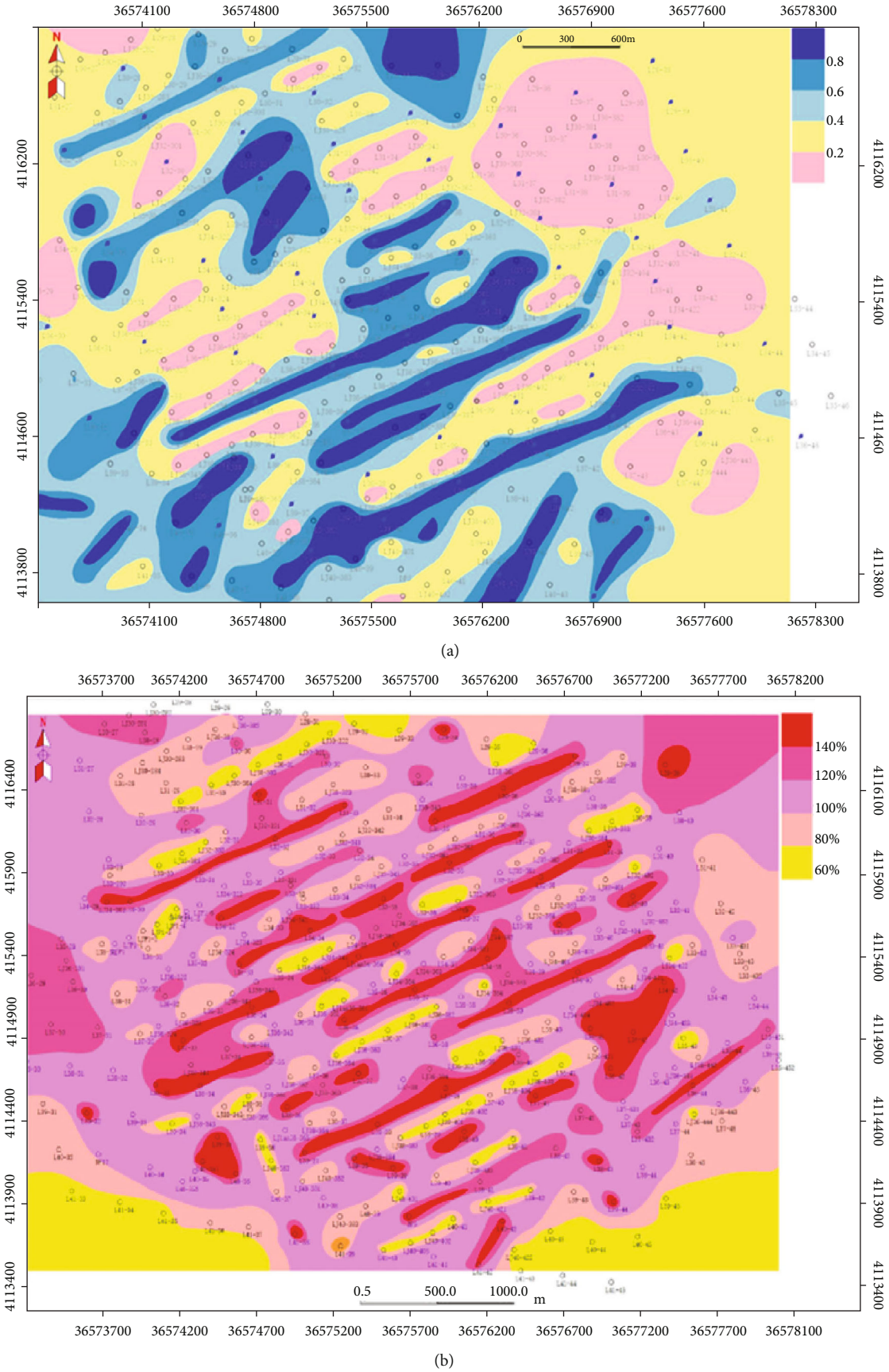

Figure 5: Schematic of (a) water cut and (b) pressure distribution of this block in 2016.

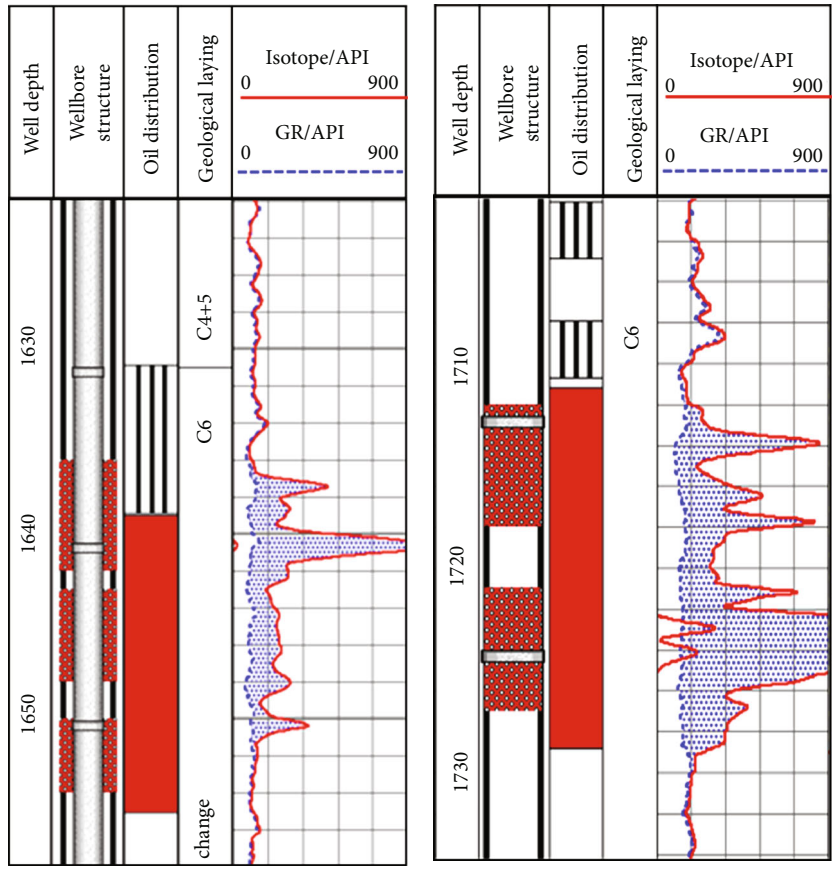

Figure 6: Typical nonuniform absorption profile of water injection wells in this block. (a) Peaking water absorption. (b) Fingering water absorption.

well L34-30 are provided in Figure 3. Obviously, this well behaves as the composite model in 2014.03, and fracture model in 2015.07, which implies the initiation of WIF. In our previous work [7], real-time monitoring, which includes modified Hall plot, evolving skin analysis, and injection/fracturing index, is used to identify the fracturing of WIFs. Different test methods are applied to investigate the uneven waterflooding performance in the vertical and areal directions. Combining the well testing analysis shown in Figure 2 and the evidences we will discuss below, we concluded that, in the most time, this fracture initiation is actually the reactivation of the original closed natural fractures in tight reservoirs. Therefore, the WIFs cannot be prevented even though the BHP is controlled below the formation breakdown pressure in the common practice. In the text below, we will focus on the evaluation of waterflooding effectiveness in this block.

3. Waterflooding Effectiveness Evaluation

3.1. Utilization Factor of Water Injection. The ideal waterflooding is to reach the uniform displacement; that is, the crude oil is displaced from the injectors towards producers by concentric circle. However, the undesired waterfloods always prevail due to the influence of reservoir heterogeneity, fractures/faults, and injection/production systems. In this block, the UF is introduced to evaluate the waterflooding efficiency, which is defined as

$$UF = \frac{W_{i(\text{ideal})}}{W_{i(\text{actual})}}, \tag{1}$$

where $W_{i(\text{actual})}$ is the actual accumulative water injection volume, $W_{i(\text{ideal})}$ is the ideal accumulative water injection volume that needed to maintain the current reservoir pressure, which may be estimated by material balance theory as

$$W_{i(\text{ideal})} = N_p B_o + W_p B_w - N B_{oi} C_t \Delta p, \tag{2}$$

and N_p is the cumulative oil production, B_o is the oil volume factor, W_p is the cumulative water production volume, B_w is the water volume factor, N is the geological reserves, B_{oi} is the initial oil volume factor, C_t is total compressibility, and Δp is the pressure difference. Using the actual production data

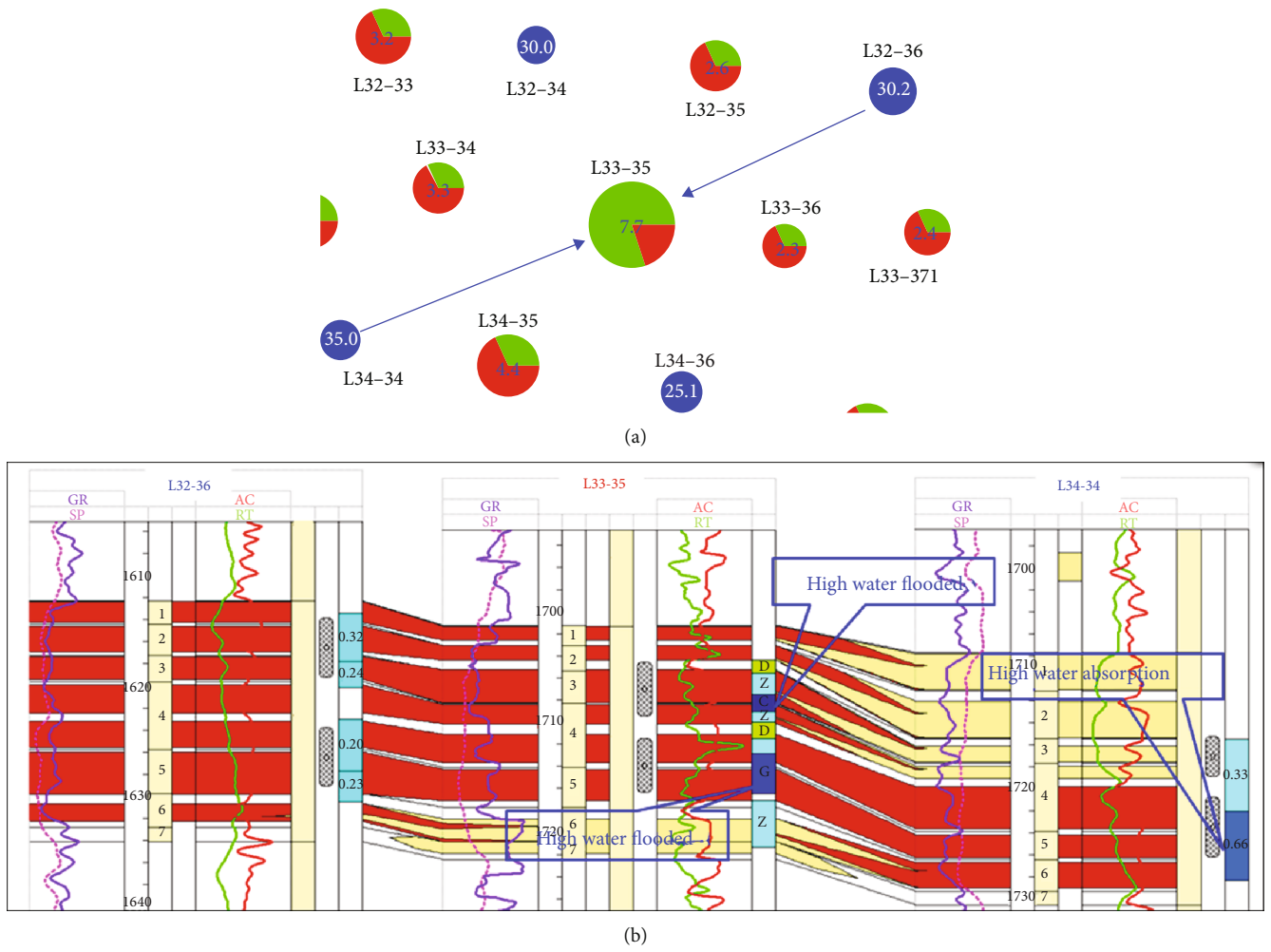

Figure 7: Behavior of production well along the maximum principal stress direction. (a) the pie chart of production of well pattern L33-35 (unit: m^3/d). (b) the vertical flooding extent of L32-36 ~ L33-35 ~ L34-34.

provided into Table 1 and the definition in Eq. (1), the UFs can be easily estimated, which are shown in the last column of Table 1 and Figure 4. The UFs from 2009 to 2016 are stable at about 1/3, which means that triple volume of water (compared with theoretical volume) is actually injected into the reservoir to maintain the current pressure. There is no clear answer on where the other 2/3 water. Some researchers guess it may be injected into ineffective formations. This low UFs of this block signify most of the water is not properly used.

3.2. Areal Sweep Characteristics. The contour map of the water cut distribution is plotted in Figure 5(a) based on the statistical results. In this figure, the deeper blue color means higher water cut. This optimal northeast-southwest waterflooding direction is in line with the maximum principal stress direction in this field. In addition, the contour map of reservoir pressure is presented in Figure 5(b), which is consistent with the water cut distribution result in Figure 5(a). These water cut and reservoir pressure distributions illustrate the highly unbalanced displacement in the areal sweep, which are validated to be caused by the influence of WIFs in our previous study [7]. The producers along the fracture direction water out quickly and unexpectedly with high pressure during the waterflooding process, while the lateral wells behave as the low production rate and pressure maintenance. For this situation, the producers along the maximum principal stress direction are suggested to convert into injectors. As a result, the areal well pattern is thus transformed into row well pattern to displace the residual oil that distributed on the both sides of WIFs.

3.3. Vertical Sweep Characteristics. Radioactive-tracer logging has been used for many years to determine the water injection profile [8, 9]. In this block, there are about 7 to 37 water injectors applied this technique every year from 2006 to 2016, and nearly half of them show the uneven displacement behaviors. The typical nonuniform water injection profiles are presented in Figure 6(a) as peaking

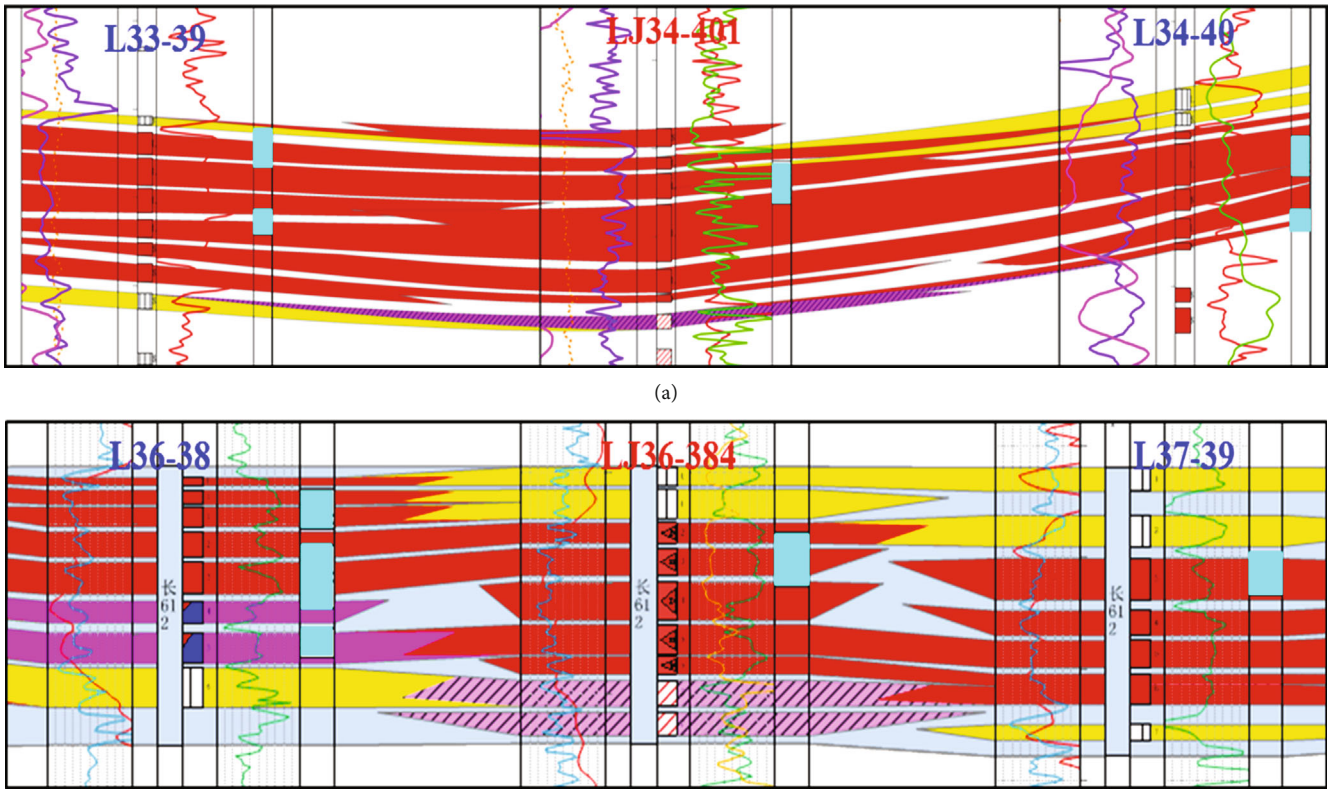

Figure 8: Section of sand body connectivity. (a) Well connected. (b) Moderate connected.

water absorption and Figure 6(b) as fingering water absorption, which may be caused by interlayer heterogeneity or WIFs. The water injection profile evolutions for a single well each year reflect the variation of relative high-permeable layers, and the special attentions should be paid for the highly absorbing layers with low flow capacity which implies the initiation of WIFs. Moderate water injection or water injection profile control is suggested to be applied to prevent the continuous extension of the induced fractures.

In addition, we also investigate the vertical sweep behavior of production wells and find that the content of vertical flooding for producers is completely different in the directions along or perpendicular to the maximum principal stress direction. There are many high water-flooded layers and large flooded areas along the maximum principal stress direction, while for the producers perpendicular to the maximum principal stress direction, the vertical water-flushed level is pretty low. Taking the Well group L33-35 as an example, the location of wells is shown in Figure 7(a), and the vertical flooding extent of L32-36 ~ L33-35 ~ L34-34 is provided in Figure 7(b). The producer L33-35 is high water flooded because it is located between injectors L34-34 and L32-36 along the maximum principal stress direction, which is generally the easiest path of WIFs' extension.

4. Key Influence Factors

4.1. Sand Body Connectivity. Sand body connectivity, which is actually depends on the distribution of sedimentary facies, is one of the main factors to influence the water-flooding performance. The sand body size, distribution, and combination characteristics are quite different in different sedimentary environments. The source direction of this block is northeast-southwest, which is approximately consistent with the maximum principal stress direction. Figure 8 demonstrates two typical examples for well and moderate connected sand body. The sand body connectivity is much better, and the thickness is much more stable along the source direction. The drainage radius of wells is limited, and the degree of sand body control by injection-production well pattern is low if it is badly connected. Therefore, the well pattern infilling may be needed to establish a better injection-production corresponding system.

4.2. Waterflood-Induced Fractures. Baker et al. [10] stated that nearly 60% of waterflood reservoirs worldwide are affected by WIFs. Due to the strong contradictions between high permeable fractures and low permeable matrix in tight reservoir, the water injection sweep efficiency is particularly low if the WIFs are formed [11, 12]. Applying the methodology proposed by Wang et al.

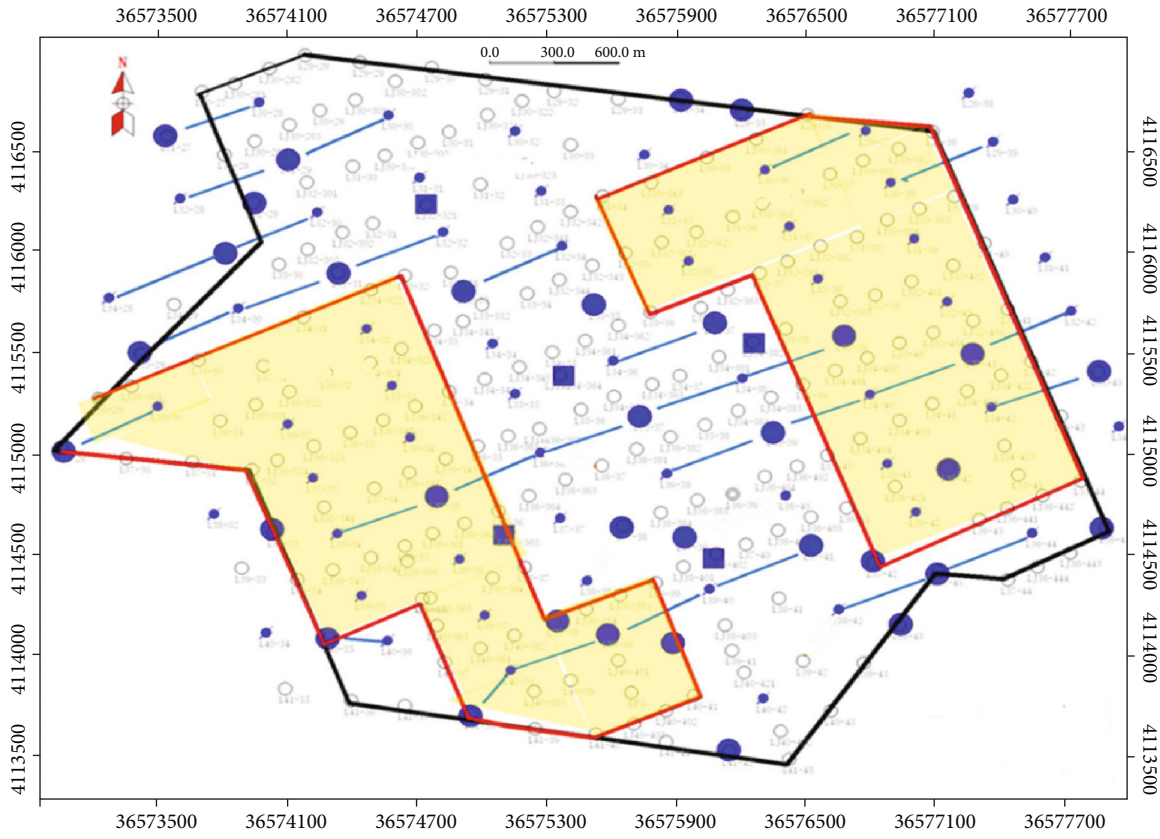

Figure 9: The distribution of WIFs in this block.

[10], we can monitor the formation plugging/fracturing timely and effectively based on the measured injection rate and THP data. Then, different formation test data are comprehensively analyzed to investigate the formation fracturing pressure and uneven waterflooding displacement in the areal and vertical directions. After that, the multiple-linear-regression or isotopic tracer method is suggested to determine the WIF directions. Based on that workflow, the WIFs are identified in this area, which is shown in Figure 9. These fractures generally distribute in the northeast-southwest direction, which is in line with the maximum principal stress direction. Generally, the producers in the WIF direction are highly water cut wells. Since the WIFs initiate and propagate gradually during the waterflood process, they cannot be easily identified during the early water injection. Once formed, they will have a great influence on water injection performance. Therefore, special attention should be paid, and the dynamic monitoring is suggested to strengthened in case of the occurrence of undesired and unexpected behaviors.

4.3. Injection and Production Correspondence. Injection and production correspondence is an another important factor that affects waterflooding performance. Take the well group L36-44 as an example. Figure 10(a) shows the pie chart of production status. The radius of the pie signifies the production rate, and the oil is marked as read; water is marked as green. The fence diagram of well pattern is demonstrated in Figure 10(b), and the water absorption profile is provided in Figure 10(c). Most of the water is absorbed in the bottom of this injector seen from Figure 10(c). The correspondences of producers L35-44, L36-45, and L37-44 with injector L36-44 are much better, which result in higher production rate, and the low production rate of well LJ36-442 is caused by the bad correspondence since it only perforates the upper oil layer. Supplementary perforation is suggested to improve the injection and production correspondence.

5. Concluding Remarks

In this paper, we propose a supplementary method of waterflooding evaluation from our previous work for the well group to field basis. The combination of UF, areal, and vertical sweep characteristic evaluation provides us an overall idea of waterflooding behavior for a field. Three main factors that largely influence the waterflooding performance in tight reservoir, including sand body connectivity, WIFs, and injection and production correspondences, are discussed. Among them, special attentions should be paid on the initiation and propagation of WIFs which are extremely important but easily ignored in the current analysis. Combining the methodology proposed in this paper and the previous study [7], managers can have a much more comprehensive and

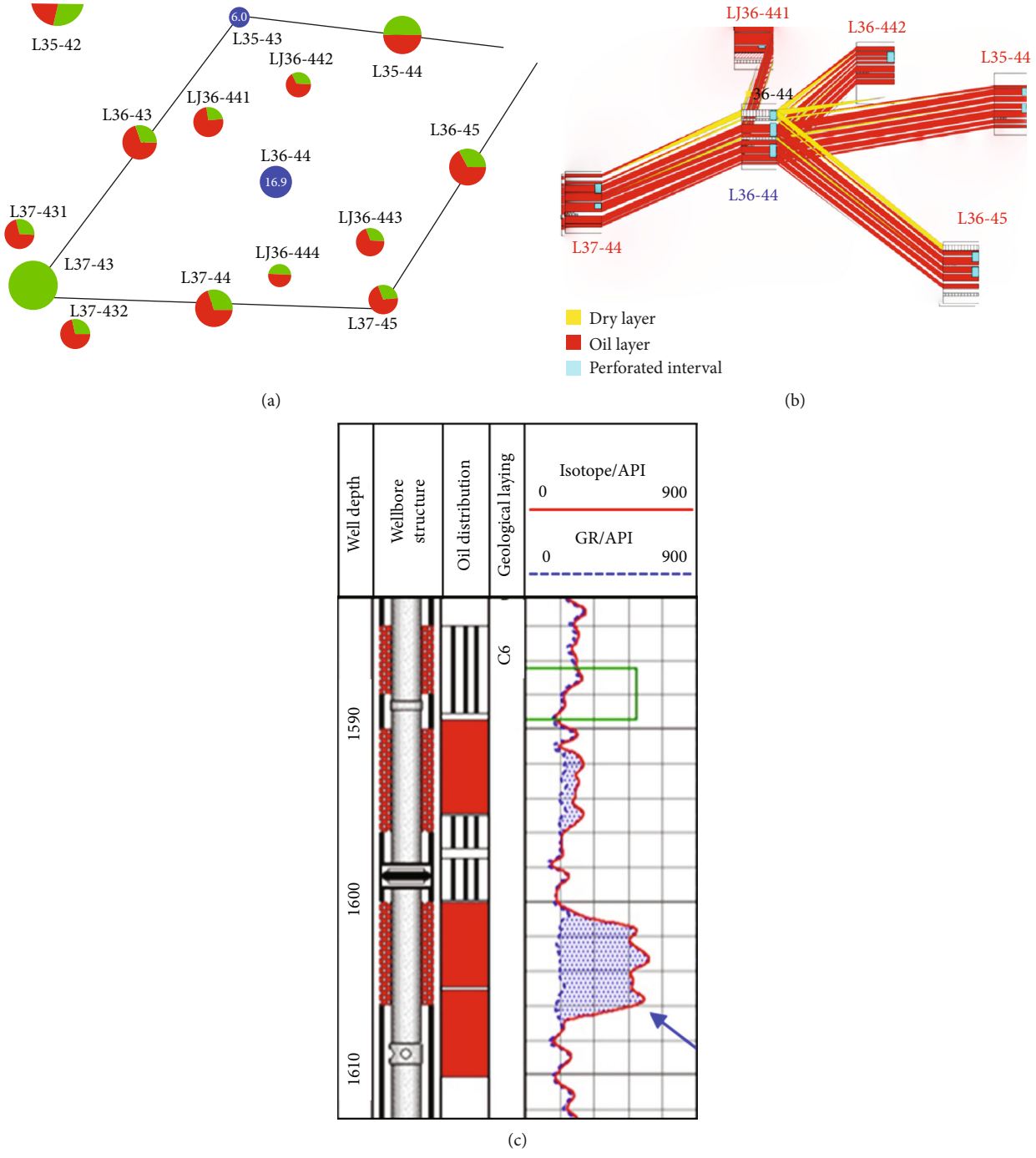

FIGURE 10: Performance of the well group L36-44. (a) Pie chart of production status. (b) Fence diagram of well pattern. (c) Water absorption profile of L36-44.

confident understanding of waterflooding performance and then make corresponding adjustment measurements to improve waterflooding effectiveness, like infill drilling, producer-injection conversion, and supplementary perforation.

Data Availability

Data is available upon requested.

Conflicts of Interest

The authors declare that they have no conflicts of interest.

Acknowledgments

The authors would like to express their thanks for the financial support from the Fundamental Research Funds for the Central Universities (2462020XKBH003) and the National Natural Science Fund of China (No. 11872073).

References

[1] M. Almarri, B. Prakasa, and D. Davies, "Identification and characterization of thermally induced fractures using modern analytical techniques," in *SPE Kingdom of Saudi Arabia Annual Technical Symposium and Exhibition*, Dammam, Saudi Arabia, 2017.

[2] B. Hustedt and J. R. R. Snippe, "Integrated data analysis and dynamic fracture modeling key to understanding complex waterfloods: case study of the Pierce Field, North Sea," *SPE Reservoir Evaluation & Engineering*, vol. 13, no. 1, pp. 82–94, 2010.

[3] Y. Wang, S. Cheng, N. Feng et al., "Semi-analytical modeling for water injection well in tight reservoir considering the variation of waterflood - induced fracture properties – case studies in Changqing Oilfield, China," *Journal of Petroleum Science and Engineering*, vol. 159, no. 2017, pp. 740–753, 2017.

[4] Y. Wang, S. Cheng, K. Zhang, and L. F. Ayala, "Investigation on the transient pressure response of water injector coupling the dynamic flow behaviors in the wellbore, waterflood-induced fracture and reservoir: semi-analytical modeling and a field case," *International Journal of Heat and Mass Transfer*, vol. 130, no. 2019, pp. 668–679, 2019.

[5] Y. He, J. Qin, S. Cheng, and J. Chen, "Estimation of fracture production and water breakthrough locations of multi-stage fractured horizontal wells combining pressure-transient analysis and electrical resistance tomography," *Journal of Petroleum Science and Engineering*, vol. 194, article 107479, 2020.

[6] F. Fang, W. Shen, X. Li, S. Gao, H. Liu, and J. Li, "Experimental study on water invasion mechanism of fractured carbonate gas reservoirs in Longwangmiao Formation, Moxi block, Sichuan Basin," *Environmental Earth Sciences*, vol. 78, no. 10, 2019.

[7] Y. Wang, S. Cheng, K. Zhang et al., "A comprehensive work flow to characterize waterflood-induced Fractures by integrating real-time monitoring, formation test, and dynamic production analysis applied to Changqing Oil Field, China," *SPE Reservoir Evaluation & Engineering*, vol. 22, no. 2, pp. 692–708, 2018.

[8] M. P. Scott, R. L. Johnson, A. Datey, C. B. Vandenborn, and R. A. Woodroof, "Evaluating hydraulic fracture geometry from sonic anisotropy and radioactive tracer logs," in *SPE Asia Pacific Oil and Gas Conference and Exhibition*, Brisbane, Qld, Australia, 2010.

[9] R. Zillur and M. Y. Al-Qahtani, "Using radioactive tracer log, production tests, fracture pressure match, and pressure transient analysis to accurately predict fracture geometry in Jauf Reservoir, Saudi Arabia," in *SPE Annual Technical Conference and Exhibition*, New Orleans, Louisiana, 2001.

[10] R. Baker, R. Dieva, R. Jobling, and C. Lok, "The myths of waterfloods, EOR floods and how to optimize real injection schemes," in *SPE Improved Oil Recovery Conference*, Tulsa, Oklahoma, 2016.

[11] B. Izgec and C. S. Kabir, "Real-time performance analysis of water-injection wells," *SPE Reservoir Evaluation & Engineering*, vol. 12, no. 1, pp. 116–123, 2009.

[12] H. A. Waheibi, S. Garimella, and W. Wardy, "Safeguarding reserves of a large carbonate waterflood field by preventing induced fractures," in *SPE Reservoir Characterization and Simulation Conference and Exhibition*, Abu Dhabi, 2013.